EMISSION OF MICROWAVES FROM InSb

Microwave emission at Q band from *n*- and *p*-type InSb subjected to applied electric and magnetic fields has been observed. Polar plots showing the dependence of the detected microwave signal on the angle between the applied electric and magnetic fields and the frequency are presented. The emission is studied at various fixed temperatures.

Microwave emission from *p*- and *n*-type InSb at 77°K in electric (E) and magnetic (H) fields has been observed at Q band (free-space wavelength = 8 mm). Electrical contacts to the semiconductor are of indium. The electric field is applied as a 0·4 μs pulse. The semiconductor, maintained at 77°K, is rectangular and lies across an evacuated waveguide terminated by a tunable short circuit. Microwaves are detected by a Q band superheterodyne. These results differ from those of Larrabee,[1] in that no emission has ever been detected for the case of E parallel to H. Work at Bell Laboratories[2] at C band showed that emission thresholds could be as low as 12 V and 45 V for *n*- and *p*-type InSb, respectively. In that experiment, emission was observed with E parallel to H.

For an etch-finished sample of *p*-type InSb (2·24 × 0·45 × 0·49 mm), with hole concentration $N_p = 2 \times 10^{13}\,\mathrm{cm}^{-3}$ at 77°K, the dependence of microwave emission (plotted radially as signal detected in volts) on the relative orientation of the constant E and H fields applied is shown in Fig. 1. The line 0–180° represents the case of E parallel to H. These curves show the single-lobed behaviour[3] (maximum signal at 90°) and the double-lobed behaviour[4] (minimum at 90°). Continuous-line traces represent emission from a pulse whose top is well defined (upper trace of Fig. 2), and dotted traces represent emission from a pulse with an unstable top (lower trace of Fig. 2). The change in character of the pulse top is a function of the electric-field value and the magnetic-field orientation, and the transition is sharply defined.

The single-lobed behaviour is reported by Suzuki[3] in experiments at X band. B. Anker-Johnson[4] reports that the emission is at minima with E and H orthogonal and parallel.

For an *n*-type sample ($N = 9 \times 10^{13}\,\mathrm{cm}^{-3}$) of size 2·38 × 0·40 × 0·38 mm, similar results to those of Fig. 1 were obtained, but the conditions for any particular form of pulse top were not nearly so clearly defined as for a *p*-type sample. Fig. 3 shows the polar dependence of the emitted signal (each trace at constant E and H) for two frequencies. The frequency difference between the two plots of Fig. 3 is 0·14 Gc/s, demonstrating that, for certain orientations of the magnetic field, microwaves whose frequencies lie in this bandwidth can be produced with more power than microwaves of frequencies in adjacent frequency bands. All previous indications have been that the emission is broadband. The existence of these frequency bands, demonstrated here with *n*-type material, is reported as occurring with *p*-type material in an abstract by B. Anker-Johnson.[4]

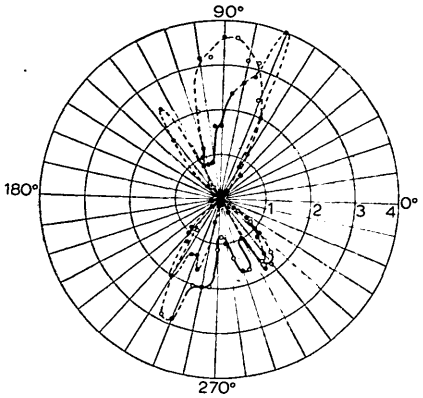

Fig. 1
H = 3·8 kGs
frequency = 34·80 Gc/s
—○— E = 8·04 × 10⁴ V/m
—●— E = 8·48 × 10⁴ V/m

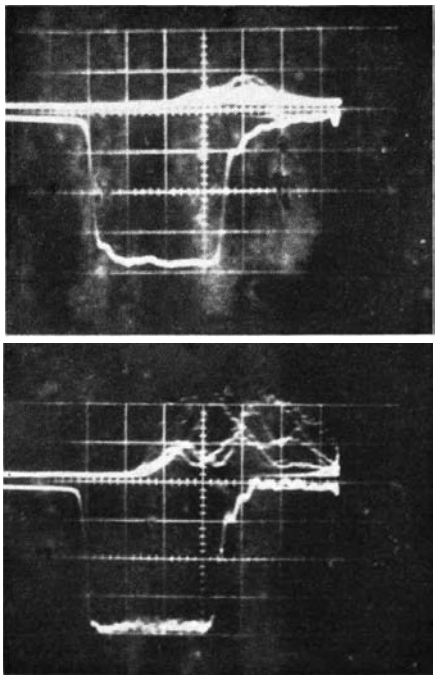

Fig. 2
H = 3·8 kGs
E and H inclined at 300°: 10 pulses
Horizontal scale: 0·1 μs/division
Top trace: vertical scale 1 V/division: microwave signal
Bottom trace: vertical scale 50 V/division: applied E pulse

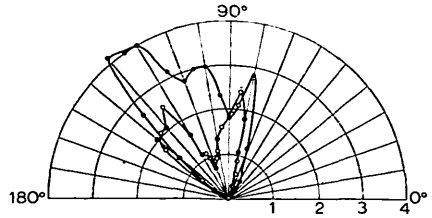

Fig. 3
H = 3·8 kGs
E = 5·05 × 10⁴ V/m
—○— 34·66 Gc/s
—●— 34·80 Gc/s

The V/i curves have been plotted for several of the relevant values of H and the orientation angle, but in these curves no discontinuity associated with the onset of microwave production can be found. For the lower values of electric fields with both *n*- and *p*-type samples, a time delay (greater than that in the measuring equipment) between the start of the E pulse and the start of the emission occurs (upper trace of Fig. 2). With higher fields the delay is substantially reduced.

Apart from the main experiments at 77°K, work with the semiconductor at 4·2°K and 90°K has shown that an emission signal can be detected equal in magnitude and with the same behaviour within the limits of error as that obtained at 77°K. At 194°K no emission has been detected.

Acknowledgment

It is a pleasure to thank Dr. B. Mullin of the Royal Radar Establishment for supplying the InSb.

L. AUCHTERLONIE *19th October 1965*

University of Oxford
Department of Engineering Science
Parks Road, Oxford, England

References

1 LARRABEE, R. D.: Proceedings of the 7th conference on semiconductors, Pt. 2, p. 181
2 BUCHSBAUM, S. J., *et al.*: *Appl. Phys. Letters*, 1965, **6**, p. 67
3 SUZUKI, K.: *Japan. J. Appl. Phys.*, 1965, **4**, p. 42
4 ANKER-JOHNSON, B.: Abstract EE12, *Bull. Amer. Phys. Soc.*, Sept. 1965, p. 720

PRACTICAL STABILITY CRITERION FOR TUNNEL-DIODE CIRCUITS

An approach is suggested to obtain a proof of the stability criterion recently proposed by McPhun. It is feared that the criterion may not be generally valid, because the phase of the reflection coefficient and bias and stabilising circuits appear to have been neglected.

An interesting stability criterion for tunnel-diode circuits has been recently proposed by McPhun.[1] Apparently it only requires plots of modulus of reflection coefficient versus real frequency. He 'derived' it intuitively. An approach to obtain a rigorous proof is offered in this communication. It is feared, however, that in certain cases the criterion may break down, because the phase of the reflection coefficient and bias and stabilising circuits appear to have been neglected.

The lossless network in Fig. 1*a* can consist, in general, of combinations of reactive and transmission-line elements. The power gain of the amplifier is the

ratio of power delivered to the load (here effectively the source) to the available power from the source. By considerations of the conservation of energy, this gain is the same[2] for any reference plane between 1 and 2 of Fig. 1*a*; it will be defined as $|\Gamma(j\omega)|^2$, where

$$\Gamma(j\omega) = \frac{Z_L(j\omega) - Z_C^*(j\omega)}{Z_L(j\omega) + Z_C(j\omega)} = \frac{N(j\omega)}{D(j\omega)} \quad (1)$$

and where Z_L and Z_C are as shown in Fig. 1.

McPhun employed the transformation $\Gamma' = -1/\Gamma$ to obtain a negative Smith chart. For stability $\Gamma(p)$ must have no right-hand p-plane poles, where $p = \alpha + j\omega$. Thus $\Gamma'(p)\{= -1/\Gamma(p)\}$ must have no right-hand p-plane zeros, and therefore $\Gamma'(j\omega)$ must encircle the origin of the $\Gamma'(j\omega)$ plane (the centre of the chart) as many times in a counterclockwise (c.c.w.) direction when ω goes from $-\infty$ to $+\infty$ as $\Gamma'(p)$ has poles in the right-hand p plane.[3] In general, the further removed the reference plane is from the diode, the more such poles there are likely to be;[4,5] all that is certain, if the exact number is unknown, is that $\Gamma'(j\omega)$ must encircle the centre of the negative Smith chart in a c.c.w. manner. Thus it is not entirely correct to say[1] that 'This curve will give no information about stability, except for the one special unstable case where at some frequency $|\Gamma|$ equals infinity.'

Since $|\Gamma(j\omega)|^2$ is independent of the reference plane chosen (what does Mr. McPhun consider to be the 'most unlikely' one?), let us consider the one nearest $-R$. The arrangement is shown in Fig. 1*b*. The diode series resistance r must be considered part of Z_L; R_0 and X are functions of ω, in general. Tentative approaches to the problem could involve the following:

(*a*) Put $d|\Gamma(j\omega)|/d\omega = 0$ to obtain ω at maximum $|\Gamma(j\omega)|$; then find the sign of $d|\Gamma(j\omega)|/dR$ for this value of ω.

(*b*) Find the sign of $d\left\{\int_0^{\omega_R} |\Gamma(j\omega)|\,d\omega\right\}/dR$, where ω_R is the resistive cutoff frequency of the diode.

(*c*) Find the sign of $d\left\{\int_{\omega_1}^{\omega_2} |\Gamma(j\omega)|\,d\omega\right\}/dR$, where the region between ω_1 and ω_2 may correspond to the amplifier bandwidth.

It is felt that a general analytic proof along these lines would be not only prohibitively difficult, but might also be unenlightening for the following reasons:

Let
$$R_S = -\frac{G}{B^2 + G^2} \quad . \quad . \quad (2)$$

$$X_S = -\frac{B}{B^2 + G^2} \quad . \quad . \quad (3)$$

where B and G are as shown in Fig. 1*b*.

For a fixed frequency,

$$\frac{dR_S}{dG} = \frac{G^2 - B^2}{(B^2 + G^2)^2} \quad . \quad . \quad . \quad (4)$$

$$\frac{dX_S}{dG} = \frac{2BG}{(B^2 + G^2)^2} \quad . \quad . \quad . \quad (5)$$

Assume, for example, that $B > G$. Then $dR_S/dG < 0$ and $dX_S/dG > 0$; i.e. as R increases, R_S increases and X_S decreases. From Fig. 2*a* it is clear that a point in quadrant 2 of the $Z(j\omega)$ plane moves nearer the origin under these conditions. Thus $|D(j\omega)|$ decreases. Since a corresponding point in a plot of $N(j\omega)$ is simply shifted to the left by $2R_0$,

$$|N(j\omega)| > |D(j\omega)| \quad . \quad . \quad . \quad (6)$$

Now

$$\frac{d|\Gamma(j\omega)|}{dR} = \frac{|D(j\omega)|\dfrac{d|N(j\omega)|}{dR} - |N(j\omega)|\dfrac{d|D(j\omega)|}{dR}}{|D(j\omega)|^2} \quad . \quad . \quad . \quad . \quad (7)$$

but

$$\frac{d|N(j\omega)|}{dR} < 0 \quad \text{and} \quad \frac{d|D(j\omega)|}{dR} < 0 \quad . \quad (8)$$

and if

$$\left|\frac{d|N(j\omega)|}{dR}\right| < \left|\frac{d|D(j\omega)|}{dR}\right| \quad . \quad (9)$$

then

$$\frac{d|\Gamma(j\omega)|}{dR} > 0 \quad . \quad . \quad (10)$$

Depending on how much greater than unity $|\Gamma(j\omega)|$ is, expr. 10 will also be true, even when expr. 9 is violated. It often occurs that the circuit is unstable when $Z_L(j\omega) + Z_C(j\omega)$ passes through quadrant 2, as there may not be one c.c.w. encirclement of the origin as a result. McPhun's criterion is valid in this case; e.g. see Fig. 2*b*: as R increases, this locus passes through the origin (gain infinite), and then becomes stable (gain falls), leading to Fig. 2*c*.

Fig. 2*d* represents a possible exception to the criterion, since $|\Gamma(j\omega)|$ could increase with R, and yet the circuit is stable. This ambiguity has arisen because the phase of $\Gamma(j\omega)$ has not been taken into account.

The tendencies for a point in the $Z(j\omega)$ plane when $B < G$ are shown in Fig. 2*e*. Fig. 2*f* shows the effect of increasing R on a tunnel-diode impedance plot $Z_D(j\omega)$; the combined effects of Figs. 2*a* and *e* are clearly demonstrated.

The plot of $Z_L(j\omega) + Z_C(j\omega)$ must start in the left-hand $Z(j\omega)$ plane for stability, since it ends in the right-hand plane, and one c.c.w. encirclement is required. The d.c. starting point tends to the left as R increases (Fig. 2*e*), so that, if the plot starts in the right-hand $Z(j\omega)$ plane, it represents an unstable circuit whose $|\Gamma(j\omega)|$ increases with R, conforming to the criterion.

Caution needs to be exercised at frequencies where the bias and stabilising circuits (which have been hitherto ignored) are effective. When they are not included as part of the 'load' of the tunnel diode, the $|\Gamma(j\omega)|$ curve will be different from when they are, depending on which side of the reference plane they happen to be and the degree of their effect. The d.c. gain in McPhun's example could not be unity when the bias circuit is accounted for; therefore his Fig. 2 does not really contain *all* the information required to indicate stability. In this case it will not be so easy to shift the reference plane.

It is hoped that this discussion will be of use in Mr. McPhun's theoretical endeavours.

J. W. BANDLER

20th October 1965

Electrical Engineering Department
Imperial College of Science and Technology
London SW7, England

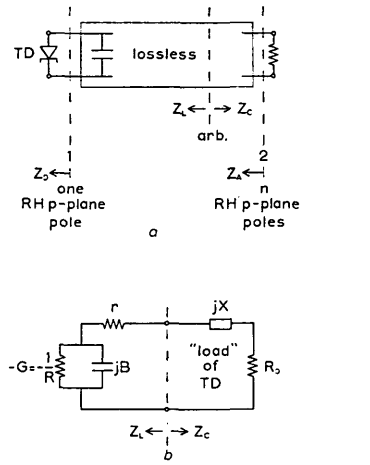

Fig. 1 *Amplifier representation*
a Choice of reference plane
b Reference plane nearest to $-R$

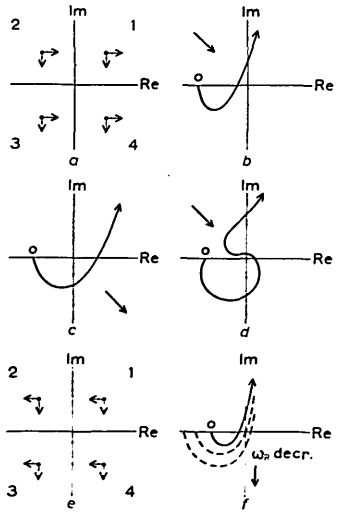

Fig. 2 *Effects in the Z(jω) plane of increasing R*
a $B > G$
b Unstable (criterion valid)
c Stable (criterion valid)
d Stable (criterion invalid)
e $B < G$
f $Z_D(j\omega)$

References

1 McPHUN, M. K.: 'Practical stability criterion for tunnel-diode circuits', *Electronics Letters*, 1965, 1, p. 167

2 CARLIN, H. J., and GIORDANO, A. B.: 'Network theory' (Prentice Hall, 1964), pp. 331–334
3 BODE, H. W.: 'Network analysis and feedback amplifier design' (Van Nostrand, 1945), p. 149
4 HENOCH, B., and KVAERNA, Y.: 'Stability criteria for tunnel-diode amplifiers', *IRE Trans.*, 1962, MTT-10, p. 397
5 BANDLER, J. W.: 'Stability and gain prediction of microwave tunnel-diode reflection amplifiers.' To be published in *IEEE Transactions on Microwave Theory and Techniques*

SERIES-FED CIRCULAR ARRAY

This letter describes how a circular array may be phased to produce a main beam in one direction by feeding the elements from a set of series-connected phase shifts. The direction of the main beam may consequently be varied by control of the values of phase shift. The significant feature of the series-feeding technique is the small phase deviation required per phase changer for 360° beam steering.

One of the most attractive features of circular antenna arrays compared with linear arrays is their ability to produce 360° of electronic beam deflection with negligible change of beam shape. On the other hand, these arrays require a more complex distribution of phase shifts round the circumference, in order to produce even the simplest forms of directional pattern. It is usually convenient to make the phase centre of the array coincident with the centre of the circle, and also to phase the elements relative to this phase centre, so that co-phasal outputs are obtained from all radiators in the main-beam direction. Such an array has a far-field directional response in the diametric plane given by

$$D(\theta) = J_0(2kR \sin \tfrac{1}{2}\theta) \quad . \quad . \quad (1)$$

where R is the circle radius, k is 2π per wavelength and θ is the observation angle relative to the main beam[1]. This letter shows that, if the elements of the array are phased relative to one element, instead of the array centre, a considerable simplification of phasing can result. The principal advantage of this arrangement is that it results in a large reduction in the peak value of the phase shifts required to form the type of directional pattern of eqn. 1, and causes it to rotate.

Fig. 1*a* shows that the electrical phase shift necessary for element r to combine all the outputs of a circular array of elements is given by

$$\gamma_r = -kR \cos(\phi_r - \theta) \quad . \quad (2)$$

where ϕ_r is the angle of the element concerned relative to some fixed reference, and θ is the direction of arrival (or transmission) of the required wavefront relative to the same fixed reference. The outputs could therefore be combined by using N phase shifters of the appropriate values $(\gamma_0, \gamma_1, \ldots \gamma_{N-1})$ connected to an N-port lossless adding network. However, it is clear from Fig. 1 that the required peak-to-peak change of phase shift is given by

$$\gamma_{p\text{-}p} = \frac{2\pi}{\lambda} \times (\text{array diameter in wavelengths}) \quad . \quad (3)$$

For large arrays this represents an inconveniently large phase deviation.

In order to deflect the beam, it is necessary to change the values of the phase shifts γ_r so that eqn. 2 is satisfied for any given direction of arrival or transmission; uniform rotation would be produced by feeding time-delayed cosinusoidal variations of phase to each element.[1] In principle, if the required peak phase excursion were too large, it would be possible to cause the phase shifters to return to zero at each multiple of 2π radians. However, this elimination of phase angles exceeding 2π would be difficult in practice, because the phase changer at each element would have to return to zero at different times (or angles). Fig. 1*b* shows a wavefront AB arriving at element 0 of an N-element circular array at an angle θ relative to the arbitrarily chosen reference axis. It is now proposed to examine the phase shifts necessary to phase the other elements to lie in phase with the signal received at element 0 from direction θ. If the phase shift required at element r is denoted by ψ_r, the values are, from Fig. 1, given by

$$\psi_0 = 0 \quad . \quad . \quad . \quad . \quad . \quad . \quad . \quad . \quad . \quad (4)$$

$$\psi_1 = kl_s \sin(\alpha + \theta) \quad . \quad . \quad . \quad . \quad . \quad (5)$$

$$\psi_2 = kl_s \sin(\alpha + \theta) + kl_s \sin(2\alpha + \theta) \quad . \quad . \quad . \quad . \quad (6)$$

$$\psi_{N-1} = kl_s \sin(\alpha + \theta) + kl_s \sin(2\alpha + \theta) + \ldots + kl_s \sin\{(N-1)\alpha + \theta\} \quad . \quad (7)$$

where l_s is the element separation in wavelengths. Examination of this series reveals that the phase shift for each element may be expressed in terms of the phase shift for the previous element plus an additional term. The elements may therefore be fed by a set of $(N-1)$ phase shifters in series, where the instantaneous values of the phase shifts are given by the differences $\psi_1 - \psi_0$, $\psi_2 - \psi_1$ etc. The important point is that the maximum phase shift required between elements is only $\pm(2\pi/\lambda)l_s$, which corresponds to the radian-length element spacing. Thus, in most cases, the peak-to-peak phase shift would always be less than 360°, independent of array diameter.[1]

If this phasing technique is to be used for electronic deflection of the directional pattern of the array, it is necessary to consider how the phase shifts vary between adjacent elements. From simple geometry it may be shown that the angle α is π/N, and invariant for any given array. The variation of the phase shifts ψ_r is therefore obtained by writing the appropriate value of θ into eqns. 4–7. It is therefore evident that, as θ varies, all the phase changers undergo identical cyclic variations of phase according to a $\sin\theta$ relationship, except that each starts from a different phase shift as indicated by the α terms in the expressions. In the case of a constant rate of rotation of the directional pattern, this is equivalent to equal progressive time lags between the cyclic variation of phase of each phase changer. One way in which it might be possible to take advantage of the phasing system just described is to consider a

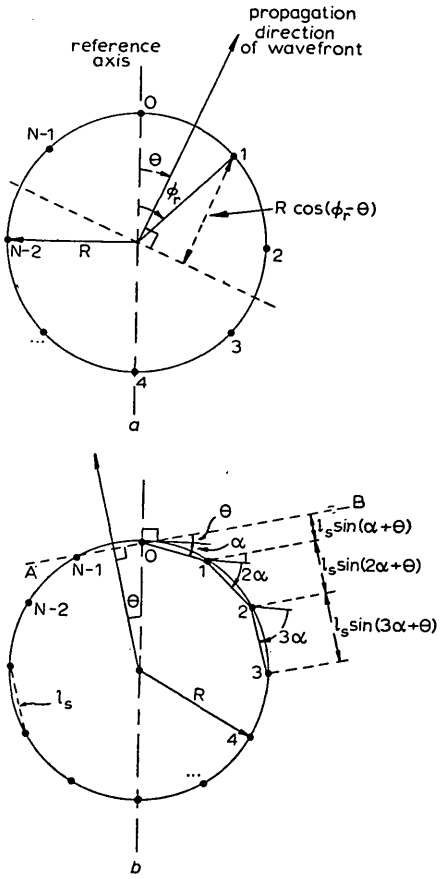

Fig. 1
a Circular-array geometry
b Geometric construction for series-fed circular array

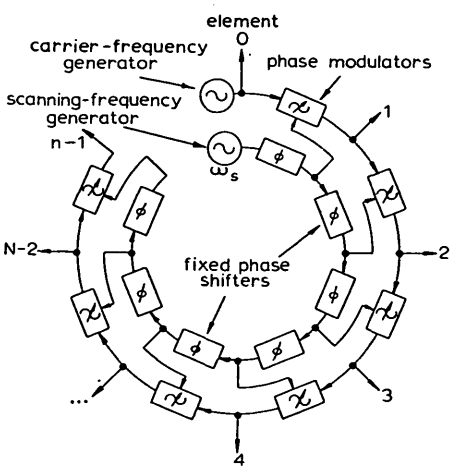

Fig. 2 *Series-fed circular-array system giving uniform electronic beam rotation*